Investigating Coastal Effects on Offshore Wind Conditions in Japan Using Unmanned Aerial Vehicles

Goto, Kazutaka
Sustainable System Research Laboratory, Central Research Institute of Electric Power Industry

Uchida, Takanori
Research Institute for Applied Mechanics (RIAM), Kyushu University

Kishida, Takeshi
Sustainable System Research Laboratory, Central Research Institute of Electric Power Industry

Nohara, Daisuke
Sustainable System Research Laboratory, Central Research Institute of Electric Power Industry

他

出版情報：Energies. 18 (5), pp.1131-, 2025-02-25. Multidisciplinary Digital Publishing Institute : MDPI
バージョン：

energies

MDPI

Article

Investigating Coastal Effects on Offshore Wind Conditions in Japan Using Unmanned Aerial Vehicles

Kazutaka Goto [1,2,*], Takanori Uchida [3], Takeshi Kishida [1], Daisuke Nohara [1], Keisuke Nakao [1] and Ayumu Sato [1]

[1] Sustainable System Research Laboratory, Central Research Institute of Electric Power Industry, 1646 Abiko, Abiko-shi 270-1166, Chiba, Japan; kisitake@criepi.denken.or.jp (T.K.); nohara@criepi.denken.or.jp (D.N.); nakao@criepi.denken.or.jp (K.N.); ayumu@criepi.denken.or.jp (A.S.)
[2] Interdisciplinary Graduate School of Engineering Sciences, Kyushu University, 6-1 Kasuga-koen, Kasuga 816-8580, Fukuoka, Japan
[3] Research Institute for Applied Mechanics (RIAM), Kyushu University, 6-1 Kasuga-koen, Kasuga 816-8580, Fukuoka, Japan; takanori@riam.kyushu-u.ac.jp
* Correspondence: ka-goto@criepi.denken.or.jp

Abstract: Wind conditions play a significant role in wind power generation. Offshore wind turbines in Japan are located in areas with a shorter fetch compared with those in Europe, raising concerns about more significant coastal effects on offshore wind conditions. Therefore, we conducted observations using unmanned aerial vehicles (UAVs) to investigate coastal effects on offshore wind conditions in Japan, measuring the vertical structure of meteorological parameters at multiple nearshore locations. We explored the application of data pre-processing methods to focus on the spatial variations caused by coastal effects and minimize short-term fluctuations. The results indicated that using ensemble averages of multiple vertical profiles effectively reduced short-term fluctuations. Our UAV observations revealed that stable stratification developed even within the 1300 m fetch region, with rapid growth rates. Additionally, we found that wind speeds were independent of height in some cases, suggesting that the wind profile power law is not suitable for expressing the vertical profiles of wind speed.

Keywords: coastal effects; nearshore wind conditions; unmanned aerial vehicle; meteorological observations; data pre-processing methods; offshore wind power

Academic Editor: Hua Li

Received: 20 December 2024
Revised: 20 February 2025
Accepted: 21 February 2025
Published: 25 February 2025

Citation: Goto, K.; Uchida, T.; Kishida, T.; Nohara, D.; Nakao, K.; Sato, A. Investigating Coastal Effects on Offshore Wind Conditions in Japan Using Unmanned Aerial Vehicles. *Energies* **2025**, *18*, 1131. https://doi.org/10.3390/en18051131

1. Introduction

In recent years, reliance on offshore wind power as a source of renewable energy has rapidly increased due to the limited supply of fossil fuels and their contribution to global warming [1,2]. Therefore, it is predicted that offshore wind power will play an increasingly important role in electricity supply in the future. However, the uncertainty and complexity of wind speed and wind power prediction influence the safety and stability of the power grid [3]. Consequently, accurately predicting wind speed and forecasting wind power is a considerable challenge.

In coastal regions, the atmospheric boundary layer experiences various changes due to complex offshore wind conditions, collectively referred to as coastal effects [4]. Offshore wind farms, particularly those located near Japan, are positioned closer to the coast (within 10 km) where these coastal effects are more pronounced compared with those in Europe [4]. Therefore, accurately identifying coastal effects is crucial for predicting wind speed and wind power in these nearshore areas.

In-situ measurements are one of the most effective methods for assessing coastal effects, particularly in understanding their effects on offshore wind conditions. However,

the installation of offshore meteorological platforms remains limited due to high costs and complex permitting processes [5]. In recent years, remote sensing systems like the Doppler wind light detection and ranging (LiDAR) have been widely used in assessing wind conditions for wind power [6,7]. The main advantage of using LiDAR (fixed laser beam geometry, looking up and forward) is its ability to examine vertical wind profiles, including at hub height, from ground-based offshore platforms. However, the high installation costs due to the offshore platforms are a disadvantage. Floating and scanning LiDAR systems (flexible geometry with adjustable laser beam azimuth and elevation angles) consist of a series of remote sensing systems without fixed offshore platforms. Floating LiDAR systems are defined as LiDAR wind-measuring devices integrated into or placed on top of a buoy [8]. Scanning LiDAR systems can scan the winds over long distances and over an entire area from the coast. Nevertheless, they are constrained by the range of the laser, which depends on the instrument model and conditions at the observation site [9,10].

Studies on coastal effects, such as low-level jets (LLJs), are primarily based on data from offshore observation campaigns, such as the FINO-WIND project [11]. Wagner et al. [12] distinguished formation mechanisms of LLJs using vertical profiles of wind speed and temperature observed at the FINO1 platforms in the southern North Sea and found that conditions such as season and upwind location influenced the formation of LLJs. Dörenkämper et al. [13] analyzed the relationships between the offshore internal boundary layer, the fetch (distance wind travels over open water), and LLJs and found that the frequency of LLJs increased with higher atmospheric stability and a shorter fetch. Among various coastal effects, the formation of LLJs is one phenomenon that influences offshore wind conditions [14]. Other coastal effects, such as the speed-up effect due to the decrease in roughness when air is advected from land to ocean, have also been reported [4,15–17]. This speed-up effect causes an increase in the Coriolis force, resulting in a slight clockwise rotation of the wind direction [18]. Coastal effects research has mainly been conducted in regions with a longer fetch, such as Europe (e.g., FINO), while less attention has been given to areas where wind farms are situated closer to the coast, such as Japan and the United States. There is a notable lack of comparative studies on offshore wind conditions in Japan [10,19], particularly regarding the development of the land-to-sea boundary layer in the nearshore region.

Hence, to address the gaps in the existing literature, we conducted two studies with the aim of developing an improved method for evaluating coastal effects and applying that method in Japan. First, we explored the suitability of unmanned aerial vehicles (UAVs) for measuring vertical meteorological profiles without requiring offshore platforms [20,21]. While UAVs have the capability to simultaneously measure multiple meteorological parameters at different nearshore locations, UAVs that do not hover provide only short-term data, which may include spatiotemporal variations [22]. Therefore, we examined the data pre-processing techniques for very short-term wind measurements taken using UAVs to investigate coastal effects. Our findings suggest that ensemble averaging of multiple UAV datasets can effectively reduce short-term fluctuations, making UAV data useful for evaluating coastal effects. Second, we conducted simultaneous meteorological observations with three UAVs in a coastal region of Japan. Each UAV measured the vertical profiles of wind speed, temperature, and humidity at different locations: onshore, 650 m offshore, and 1300 m offshore. Our analysis of these vertical profiles near the coast indicated the development of stable stratification as the fetch increased from land to ocean. In this study, data analysis was performed using Python (version 3.10.6). Python is available at (https://www.python.org, accessed on 20 February 2025).

2. Study Setup for the Analysis of Coastal Effects

2.1. Study Area

In this study, we collected observational data from the coastal region of Noshiro, Japan. The location of the observation site and the outline of the measurements are shown in Figure 1. This coastal area is a port, and the surrounding land is flat. The Ministry of Economy, Trade, and Industry in Japan designated the coastal region of Noshiro as an area for the promotion of offshore renewable energy facilities [23], and several wind turbines are located in this region within a few kilometers offshore.

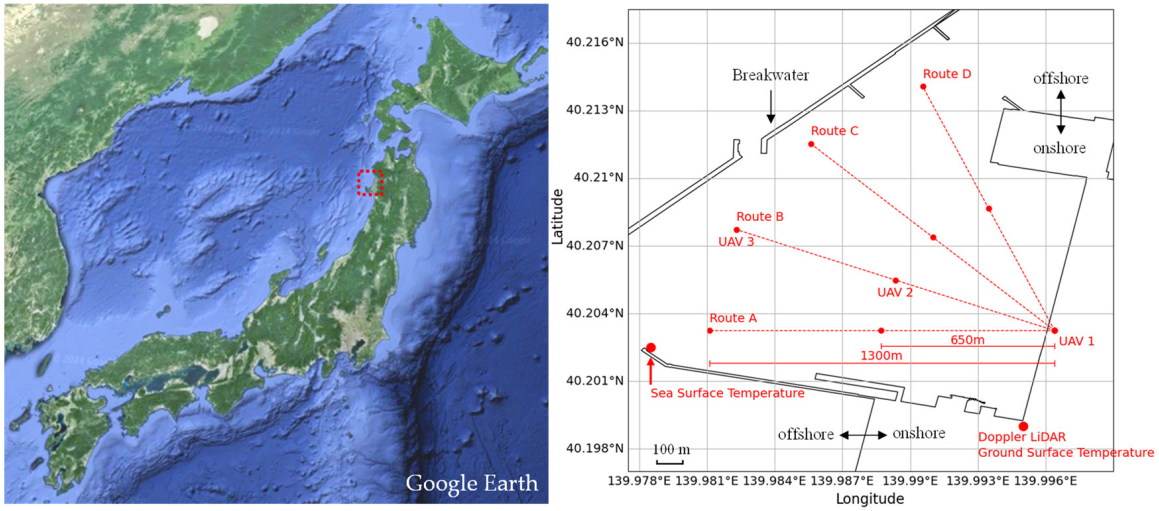

(**a**) (**b**)

Figure 1. Overview of the observation site and outline: (**a**) location of the observation site (Noshiro, Japan), with the red frame showing Noshiro; (**b**) outline of the measurements.

2.2. Equipment

In this study, we conducted simultaneous observations using three UAVs (Figure 2). We used PF2 UAV bodies (ACSL Ltd., Tokyo, Japan) and installed attachments for measuring meteorological parameters (Table 1). All the three UAVs were of the same type and were equipped with identical attachments.

Figure 2. The unmanned aerial vehicle (UAV) body and installed attachments.

Table 1. Summary of UAV body and attachment specifications.

Body and Attachments	Specifications
UAV body	Height: 536 mm Total weight: 7.1 kg Max payload: 2.75 kg Wind resistance: 10 m/s Battery: 12,000 mAh × 2
Ultrasonic wind sensor	WXT532 made by Vaisala (Vantaa, Finland) Accuracy: ±3% (in 10 m/s)
Thermal sensor	NFR C3-0508-30 made by Netsushin (Saitama, Japan) Accuracy: ±0.3 K Forced ventilation and a filter covering the sensor to avoid direct solar radiation

Note: UAV, unmanned aerial vehicle.

2.3. Methodology

Each of the three UAVs measured the vertical profiles of wind speed, temperature, and humidity at different points: onshore, 650 m offshore, and 1300 m offshore. Additionally, the collected data from each UAV included three vertical profiles observed during a single flight. Among the collected data, that during the ascent (at a rate of 1.5 m/s) was used, while that during descent was not used due to the influence of the UAV's wake. Routes A–D (Figure 1) were selected based on the upper wind direction immediately before each flight, with the aim of positioning the three UAVs as closely aligned with the wind direction as possible. In addition to the UAVs, a profiling LiDAR was installed 500 m horizontally from the onshore UAV flight point. The upper wind data collected using LiDAR were used to select the flight route. Observations were conducted during 13–18 September 2023. The upper wind directions (100 m altitude) and flight durations are shown in Figure 3. During the observation period, the land–sea breeze circulations were clearly observed, specifically the land breeze in the early morning and the sea breeze that followed. However, the sea and land breezes were not exactly 180° opposite, probably due to the influence of surrounding structures or topography.

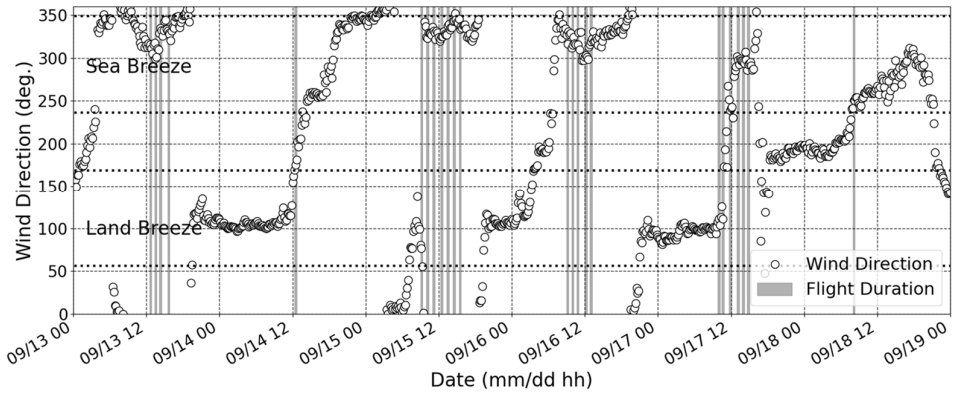

Figure 3. The upper wind directions at an altitude of 100 m and flight durations, measured using LiDAR.

2.4. UAV Data Processing Techniques

A major advantage of UAVs is their ability to measure meteorological vertical profiles without the need for offshore platforms. However, UAVs that do not hover provide only short-term data. When detecting coastal effects, such as LLJs or wind shear, the vertical wind speed profile is typically derived from data averaged over 10–20 min [12,24]. However, UAVs generate data with time lags between altitudes due to their ascent. In

this study, as the UAVs ascended at a rate of 1.5 m/s, reaching approximately 250 m in altitude, it took approximately 167 s to complete a single vertical profile. This time lag complicates the determination of whether vertical wind speed differences result from the vertical atmospheric structure influenced by coastal effects or from wind speed fluctuations. To address these issues, we explored two data pre-processing methods to minimize short-term fluctuations.

Figure 4 illustrates the vertical moving average data pre-processing technique, which uses five-point up–down data to minimize short-term fluctuations. In this study, as the UAVs ascended at a rate of 1.5 m/s and collected meteorological data at 1 s intervals, the vertical moving average was calculated using data within a vertical range of ±3.75 m. Additionally, a weighted coefficient was not used for the vertical moving average. The second method we explored was an ensemble averaging of three vertical profiles. Figure 5 illustrates one example of the time schedule for UAV data collection, showing three vertical profiles (V1–V3) used for ensemble averaging, along with the 10-min averaging period for the LiDAR data, ensuring the closest possible time alignment. The LiDAR-derived wind speeds, averaged over a 10-min period, were compared with UAV wind speeds measured onshore (UAV1).

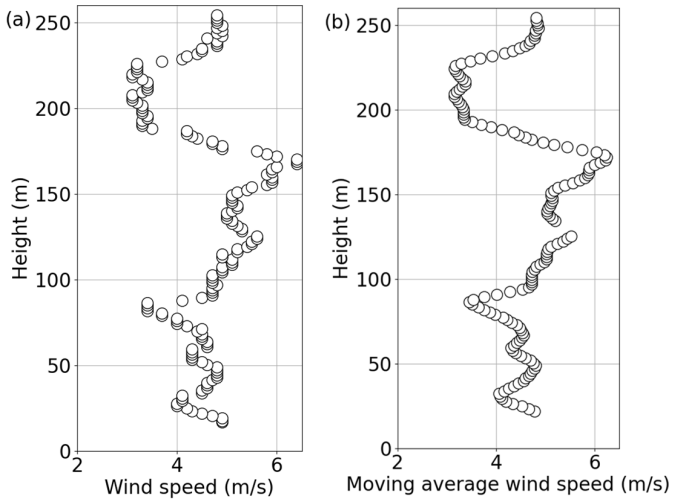

Figure 4. Vertical profiles of wind speed flight durations: (**a**) raw data and (**b**) moving average wind speed.

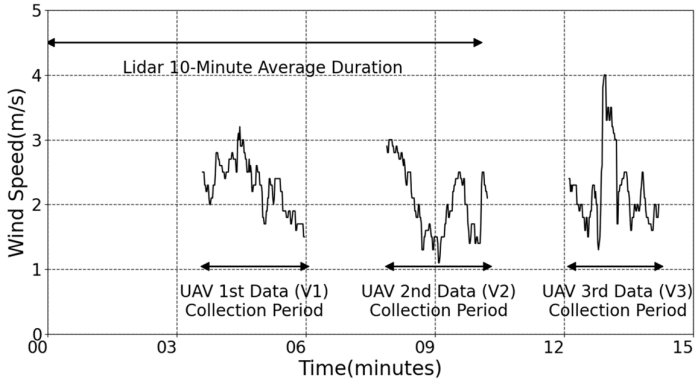

Figure 5. An example of the time schedule for UAV data collection, illustrating three vertical profiles (V1–V3) used for ensemble averaging, along with the 10-min averaging period for the LiDAR data, ensuring the closest possible time alignment.

3. Results

3.1. Analysis of UAV Data Processing

Figure 6 shows the comparison of wind speeds measured using the onshore UAV with those measured using LiDAR. As the LiDAR was installed 500 m horizontally from the onshore UAV flight point, data from the highest available range (140–240 m) were used for the comparison to minimize the local effects of buildings and coastal forests near the ground surface. Each subplot displays averaged wind speeds from UAVs using no averaging, the vertical moving average, the ensemble averaging of vertical profiles, or both methods and compares them with LiDAR wind speeds averaged over a 10-min period. Based on qualitative analysis, the ensemble-averaged wind speeds (Vall) showed less variability and better agreement with LiDAR wind speeds than the individual flight data (V1–V3). The coefficient of determination and root mean square error scores also supported these findings. However, the moving-averaged wind speeds showed less variability based on qualitative perspectives. Nevertheless, the scores showed little improvement. In the case of V3, within the range of high wind speeds (>8 m/s), the UAV wind speeds were higher than those measured using LiDAR. This implies short-term wind speed fluctuations. Despite this, the Vall wind speeds showed better agreement with the LiDAR wind speeds when averaged over a 10-min period. This suggests that ensemble averaging of vertical profiles minimizes short-term fluctuations. Thus, in measuring wind speeds with short-term fluctuations, such as in V3, a single UAV flight may provide different results from LiDAR in detecting coastal effects. Additionally, relying on single-flight data complicates the determination of whether vertical wind speed differences result from the vertical atmospheric structure under the influence of coastal effects or from wind speed fluctuations due to time lags between lower and upper layers, which are affected by turbulence. To address these issues, we demonstrated that ensemble averaging of vertical profiles is effective.

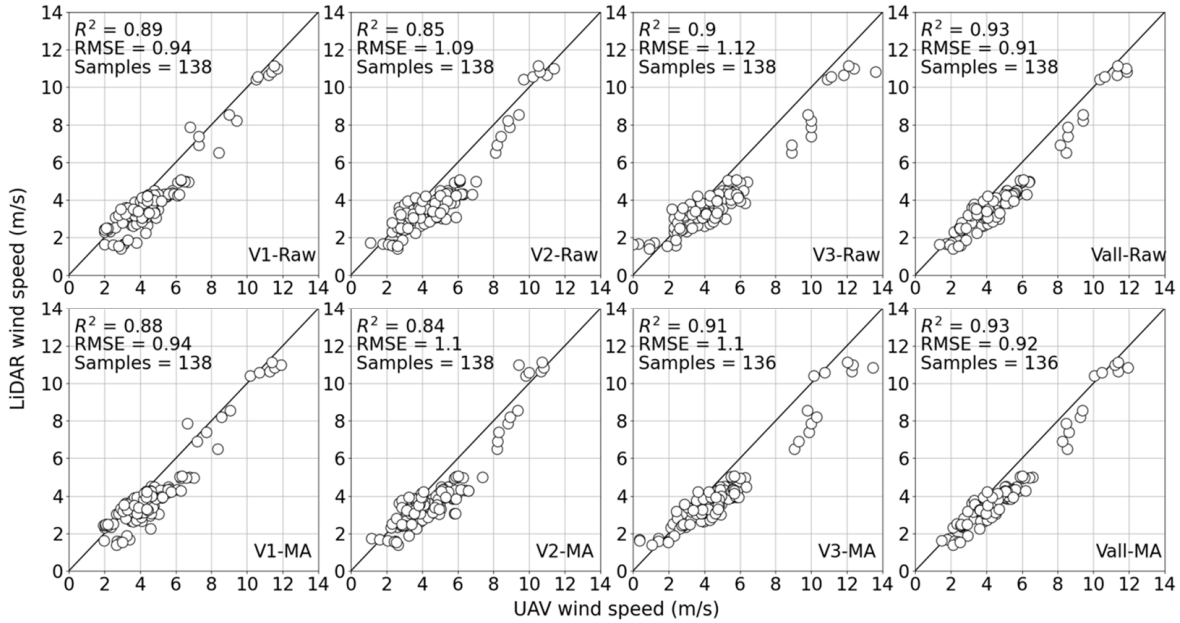

Figure 6. The comparison of wind speeds measured using onshore UAV with those measured using LiDAR. Note: V1–V3: individual flight data, Vall: ensemble-averaged wind speeds, Raw: wind speeds of raw data, and MA: moving-averaged wind speeds.

Wind shear is among the coastal effects caused by stable stratification [16]. High-quality data are required to evaluate wind shear accurately. Figure 7 shows the comparison of wind shear coefficients [12] measured using UAVs with those measured using LiDAR.

The wind shear coefficient was expressed as the ratio of the wind speed at 240 m to the wind speed at 140 m. The results shown in Figures 6 and 7 support the effectiveness of ensemble averaging. Additionally, the vertical moving average shows less variability and better scores (the coefficient of determination and root mean square error scores) than the raw data. However, in the case of V2, only the vertical moving average (V2-MA) was inadequate for correcting an outlier. In contrast, this outlier was corrected in the ensemble averaging (Vall).

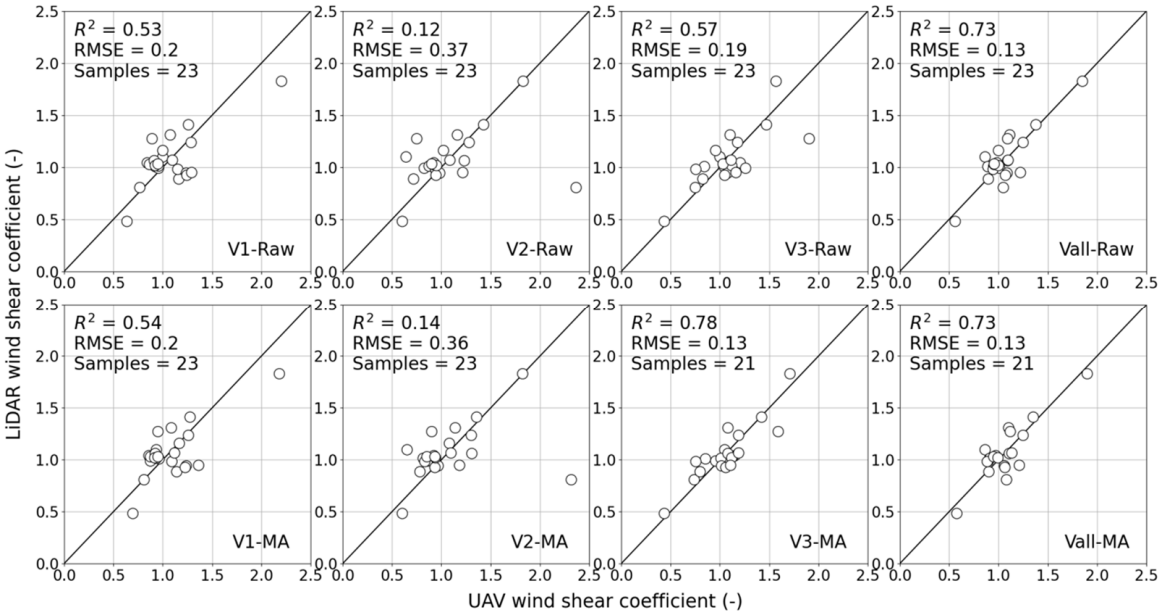

Figure 7. Comparison of wind shear coefficients measured using UAVs with those measured using LiDAR.

3.2. Vertical Atmospheric Structures in the Coastal Region of Japan

In this phase, the results of investigating coastal effects on offshore wind conditions were reported. Figure 8 shows the vertical profiles of potential temperature with the internal boundary layer height (IBLH), which is defined using a simple empirical equation [4,25], for land breeze conditions. The empirical equation was proposed to describe the dependence of the IBLH (h) on the fetch (x) and the temperature difference ($\Delta\theta$) between the sea and land. The equation is as follows:

$$h(x) = au(g\Delta\theta/\theta)^{-1/2}x^{1/2}, \quad (1)$$

where u is wind speed, g is gravitational acceleration, θ is ocean temperature, and a is a constant value based on observations and simulations [25], ranging between 0.014 and 0.024. The IBLH was calculated using a simple empirical equation, based on observed parameters. The case in Figure 8 shows positive gradients of potential temperature at altitudes near the sea surface due to its cooling effect. However, compared to observations, the empirical equation underestimates the IBLH. This implies that the growth rate of the IBLH is faster in the observations than in the results of the empirical equation. One possible reason for this difference may be the influence of coastal protection forests and structures, such as the shape of seawalls and the arrangement of buildings, on local meteorological conditions; these factors are not accounted for in the empirical equation. However, more detailed data, such as spatial distribution, are required to clarify this factor.

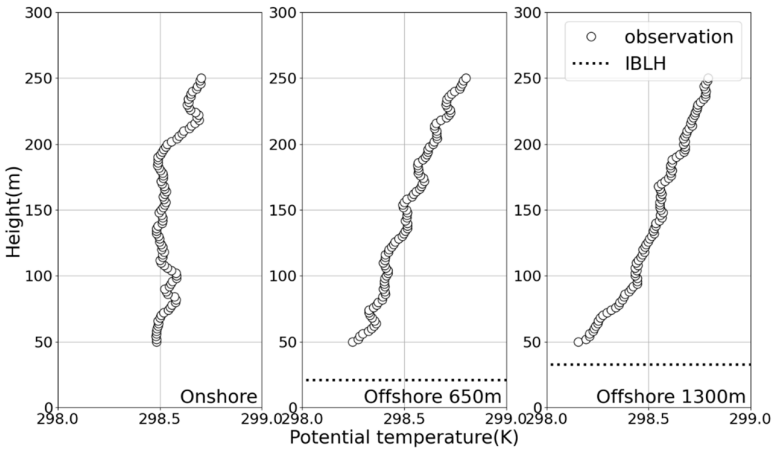

Figure 8. Vertical profiles of potential temperature with the internal boundary layer height (IBLH), which was calculated using a simple empirical equation, based on observed parameters, on 17 September 2023, at 09:50 (local time).

Figure 9 shows the vertical profiles of potential temperature differences between two altitudes separated by 70 m at different points: onshore, 650 m offshore, and 1300 m offshore. Each vertical profile was classified as either a land breeze or sea breeze sector based on the upper wind direction measured using LiDAR, and then averaged within each sector. Even within the 1300 m fetch region, we found that stable stratification became noticeably stronger as the fetch increased. Additionally, this phenomenon was clearly observed in the land breeze sectors. The stable stratification is known to cause coastal effects, such as LLJs, which influence offshore wind conditions [13]. However, no clear coastal effects were observed in the wind speed profiles during the period when stable stratification developed from our measured data specifically. One reason for this discrepancy could be that the potential temperature differences are smaller compared to the differences observed during LLJs in Europe (in this study, the maximum value observed was 0.5 K) [13]. Consequently, additional observations are needed under different conditions, such as during seasons with larger differences between the land and sea surface temperatures.

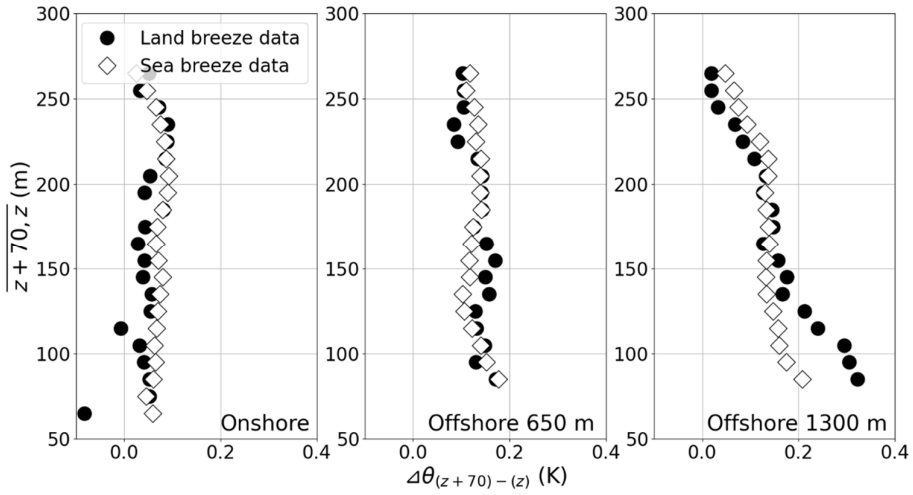

Figure 9. Vertical profiles of potential temperature differences between altitudes at different points. Note: z: the lower height level used to calculate the plot data (the 70 m average), θ: potential temperature (K).

The wind speed (V) at height (z) is expressed using the exponent α, as follows:

$$V(z) = V(z_r) \cdot \left(\frac{z}{z_r} \right)^{\alpha}, \quad (2)$$

where z_r is the reference height (50 m). The exponent α is calculated by fitting the empirical Equation (2) to the observed vertical profiles of wind speed using the least squares method. The results are shown in Figure 10. The exponent α showed very low values regardless of location (onshore, 650 m offshore, or 1300 m offshore). The average values were below 0.1, which is lower than the values of observations in Mutsu-Ogawara, Japan [19]. These results showed not only low but also negative values of the exponents, which indicates that wind speeds were independent of height in some cases, suggesting that the wind profile power law is not suitable for expressing the vertical profiles of wind speed.

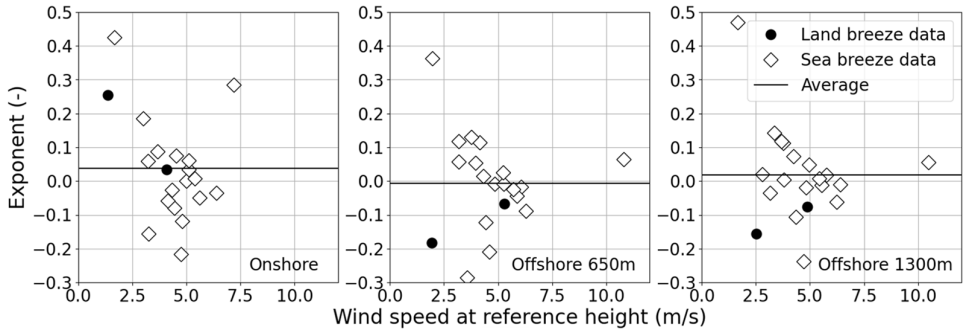

Figure 10. The exponents of the wind profile power law.

4. Discussion

In this study, we investigated offshore wind conditions in Japan. We used three UAVs to observe the vertical profiles of wind speed and temperature at different locations: onshore, 650 m offshore, and 1300 m offshore. Additionally, we compared the features of UAV and LiDAR observations and explored data pre-processing methods.

We focused on how to reduce the spatiotemporal variations in the short-term data collected using UAVs and the observation plans needed for this purpose. These variations make the analysis of coastal effects on offshore wind conditions difficult without further processing. Our study demonstrated that data pre-processing, especially using the ensemble average, was effective in minimizing short-term fluctuations. It is important to collect several vertical profiles during a UAV flight to investigate the influence of coastal effects on offshore wind conditions. Our findings suggest that UAV observations are effective for the analysis of coastal effects on offshore wind conditions. Although UAVs can measure high-resolution spatial data at different points, they are not capable of capturing long-term data due to the limitations in flight duration imposed by battery life, which is a disadvantage of UAVs when compared with LiDAR and offshore meteorological towers. Therefore, UAVs may be most suitable for conducting temporary observations at locations where long-term observations are also conducted. For example, UAV-observed data could be combined with meteorological tower data to investigate the influence of coastal effects on offshore wind conditions.

To our knowledge, this is the first study to investigate the vertical profiles of potential temperature in nearshore areas in Japan using UAVs. The vertical profiles showed stable stratification offshore, similar to previously reported data from Europe [4]. However, the potential temperature differences between the two altitudes were smaller compared with the differences observed during LLJs in Europe [13], and the effect of the stable stratification on offshore wind conditions was not clearly confirmed. Therefore, further observations

are required under different conditions, such as seasons with larger potential temperature differences and over long-term periods. In the vertical profiles of potential temperature at different distances from the shore, we observed that stable stratification became noticeably stronger as the fetch increased. These results were compared to the IBLH calculated using an empirical equation [4,25], which revealed that the observed IBLH grew at a much faster rate as the fetch increased than that calculated using the empirical equation. Additionally, we determined that the exponent α calculated from observed wind speed data in our study was lower than the observed values in Mutsu-Ogawara, Japan [19]. Moreover, we found that the observed wind speeds were independent of height and that the power law is not suitable for expressing wind speed in some cases. Our observations were conducted nearshore under specific seasonal and daytime conditions; therefore, further observations under different conditions are required for a more comprehensive analysis.

Author Contributions: Conceptualization, K.G. and T.U.; methodology, K.G., T.U., T.K., D.N. and K.N.; software, K.G.; validation, K.G.; formal analysis, K.G.; investigation, K.G. and T.K.; resources, T.K. and A.S.; data curation, K.G.; writing—original draft preparation, K.G.; writing—review & editing, K.G., T.U., T.K., D.N., K.N. and A.S.; visualization, K.G.; supervision, T.U., T.K., D.N. and A.S.; project administration, K.G. and A.S.; funding acquisition, K.G. and A.S. All authors have read and agreed to the published version of the manuscript.

Funding: This research received no external funding.

Data Availability Statement: The corresponding author can provide the data presented in this study upon request.

Conflicts of Interest: The authors declare that there are no potential conflicts of interest.

References

1. Wang, J.; Song, Y.; Liu, F.; Hou, R. Analysis and application of forecasting models in wind power integration: A review of multi-step-ahead wind speed forecasting models. *Renew. Sustain. Energy Rev.* **2016**, *60*, 960–981. [CrossRef]
2. Yang, B.; Yu, T.; Shu, H.; Dong, J.; Jiang, L. Robust sliding-mode control of wind energy conversion systems for optimal power extraction via nonlinear perturbation observers. *Appl. Energy* **2018**, *210*, 711–723. [CrossRef]
3. Holttinen, H.; Kiviluoma, J.; Forcione, A.; Milligan, M.; Smith, J.C.; Dobschinski, J.; van Roon, S.; Dillon, J.; Cutululis, N.; Orths, A.; et al. *Design and Operation of Power Systems with Large Amounts of Wind Power*; NREL/TP-5D00-66596; VTT Tiedotteita Valtion Teknillinen Tutkimuskeskus: Espoo, Finland; USDOE Office of Energy Efficiency and Renewable Energy (EERE), Wind and Water Technologies Office (EE-4W): Washington, DC, USA, 2009. Available online: https://iea-wind.org/wp-content/uploads/2021/08/T268.pdf (accessed on 3 December 2024).
4. Schulz-Stellenfleth, J.; Emeis, S.; Dörenkämper, M.; Bange, J.; Cañadillas, B.; Neumann, T.; Schneemann, J.; Weber, I.; zum Berge, K.; Platis, A.; et al. Coastal impacts on offshore wind farms—A review focussing on the German Bight area. *Meteorol. Z.* **2022**, *31*, 289–315. [CrossRef]
5. Archer, C.L.; Colle, B.A.; Delle Monache, L.; Dvorak, M.J.; Lundquist, J.; Bailey, B.H.; Beaucage, P.; Churchfield, M.J.; Fitch, A.C.; Kosovic, B.; et al. Meteorology for coastal/offshore wind energy in the United States: Recommendations and research needs for the next 10 years. *Bull. Amer. Meteorol. Soc.* **2014**, *95*, 515–519. [CrossRef]
6. Hasager, C.; Stein, D.; Courtney, M.; Peña, A.; Mikkelsen, T.; Stickland, M.; Oldroyd, A. Hub height ocean winds over the North Sea observed by the NORSEWInD lidar array: Measuring techniques, quality control and data management. *Remote Sens.* **2013**, *5*, 4280–4303. [CrossRef]
7. Clifton, A.; Clive, P.; Gottschall, J.; Schlipf, D.; Simley, E.; Simmons, L.; Stein, D.; Trabucchi, D.; Vasiljevic, N.; Würth, I. IEA wind Task 32: Wind lidar identifying and mitigating barriers to the adoption of wind lidar. *Remote Sens.* **2018**, *10*, 406. [CrossRef]
8. Gottschall, J.; Wolken-Möhlmann, G.; Viergutz, T.; Lange, B. Results and conclusions of a floating-lidar offshore test. *Energy Procedia* **2014**, *53*, 156–161. [CrossRef]
9. Rott, A.; Schneemann, J.; Theuer, F.; Trujillo Quintero, J.J.; Kühn, M. Alignment of scanning lidars in offshore wind farms. *Wind Energy Sci.* **2022**, *7*, 283–297. [CrossRef]
10. Shimada, S.; Goit, J.P.; Ohsawa, T.; Kogaki, T.; Nakamura, S. Coastal wind measurements using a single scanning LiDAR. *Remote Sens.* **2020**, *12*, 1347. [CrossRef]

11. Deutscher Wetterdienst (DWD). The FINO-WIND Project. Available online: https://www.dwd.de/EN/research/projects/fino_wind/fino_wind_en_node.html (accessed on 19 August 2024).
12. Wagner, D.; Steinfeld, G.; Witha, B.; Wurps, H.; Reuder, J. Low level jets over the southern North Sea. *Meteorol. Z.* **2019**, *28*, 389–415. [CrossRef]
13. Dörenkämper, M.; Optis, M.; Monahan, A.; Steinfeld, G. On the offshore advection of boundary-layer structures and the influence on offshore wind conditions. *Bound. Layer Meteorol.* **2015**, *155*, 459–482. [CrossRef]
14. Gadde, S.N.; Stevens, R.J.A.M. Effect of low-level jet height on wind farm performance. *J. Renew. Sustain. Energy* **2021**, *13*, 013305. [CrossRef]
15. Taylor, P.A. On wind and shear stress profiles above a change in surface roughness. *Q. J. R. Meteorol. Soc.* **1969**, *95*, 77–91. [CrossRef]
16. Barthelmie, R.J.; Palutikof, J.P. Coastal wind speed modelling for wind energy applications. *J. Wind Eng. Ind. Aerodyn.* **1996**, *62*, 213–236. [CrossRef]
17. Lange, B.; Larsen, S.; Højstrup, J.; Barthelmie, R. Importance of thermal effects and sea surface roughness for offshore wind resource assessment. *J. Wind Eng. Ind. Aerodyn.* **2004**, *92*, 959–988. [CrossRef]
18. Emeis, S.; Harris, M.; Banta, R.M. Boundary-layer anemometry by optical remote sensing for wind energy applications. *Meteorol. Z.* **2007**, *16*, 337–347. [CrossRef]
19. Konagaya, M.; Ohsawa, T.; Inoue, T.; Mito, T.; Kato, H.; Kawamoto, K. Land–sea contrast of nearshore wind conditions: Case study in Mutsu-Ogawara. *Sola* **2021**, *17*, 234–238. [CrossRef]
20. Shimura, T.; Inoue, M.; Tsujimoto, H.; Sasaki, K.; Iguchi, M. Estimation of wind vector profile using a hexarotor unmanned aerial vehicle and its application to meteorological observation up to 1000 m above surface. *J. Atmos. Ocean. Technol.* **2018**, *35*, 1621–1631. [CrossRef]
21. Sasaki, K.; Inoue, M.; Shimura, T.; Iguchi, M. In situ, rotor-based drone measurement of wind vector and aerosol concentration in volcanic areas. *Atmosphere* **2021**, *12*, 376. [CrossRef]
22. Van der Hoven, I. Power spectrum of horizontal wind speed in the frequency range from 0.0007 to 900 cycles per hour. *J. Meteorol.* **1957**, *14*, 160–164. [CrossRef]
23. Ministry of Economy, Trade and Industry. Available online: https://www.meti.go.jp/english/index.html (accessed on 19 August 2024).
24. Debnath, M.; Doubrawa, P.; Optis, M.; Hawbecker, P.; Bodini, N. Extreme wind shear events in US offshore wind energy areas and the role of induced stratification. *Wind Energy Sci.* **2021**, *6*, 1043–1059. [CrossRef]
25. Garratt, J.R. *The Atmospheric Boundary Layer*; Cambridge University Press: Cambridge, UK, 1992.